



## Soil carbon dioxide emissions due to oxidative peat decomposition in an oil palm plantation on tropical peat

Kiwamu Ishikura<sup>a,\*</sup>, Takashi Hirano<sup>a</sup>, Yosuke Okimoto<sup>a</sup>, Ryuichi Hirata<sup>b</sup>, Frankie Kiew<sup>a,c</sup>, Lulie Melling<sup>c</sup>, Edward Baran Aeries<sup>c</sup>, Kim San Lo<sup>c</sup>, Kevin Kemudang Musin<sup>c</sup>, Joseph Wenceslaus Waili<sup>c</sup>, Guan Xhuan Wong<sup>a,c</sup>, Yoshiyuki Ishii<sup>d</sup>

<sup>a</sup> Research Faculty of Agriculture, Hokkaido University, Kita-ku, Kita 9, Nishi 9, Sapporo, Hokkaido, 060-8589, Japan

<sup>b</sup> Center for Global Environmental Research, National Institute for Environmental Studies, Tsukuba, Ibaraki, 305-8506, Japan

<sup>c</sup> Sarawak Tropical Peat Research Institute, Lot 6035, Kuching, Kota Samarahan Expressway, 94300, Kota Samarahan, Sarawak, Malaysia

<sup>d</sup> Institute of Low Temperature Science, Hokkaido University, Kita-ku, Kita 19, Nishi 8, Sapporo, Hokkaido, 060-0819, Japan

### ARTICLE INFO

#### Keywords:

Automated chamber system  
Carbon dioxide efflux  
Groundwater level  
Heterotrophic respiration  
Soil respiration  
Subsidence  
Trenching

### ABSTRACT

Soil carbon dioxide (CO<sub>2</sub>) efflux was measured continuously for two years using an automated chamber system in an oil palm plantation on tropical peat. This study investigated the factors controlling the CO<sub>2</sub> efflux and quantified the annual cumulative CO<sub>2</sub> emissions through soil respiration and heterotrophic respiration, which is equivalent to oxidative peat decomposition. Soil respiration was measured in close-to-tree (< 2.5 m, CT) and far-from-tree (> 3 m, FT) plots, and heterotrophic respiration was measured in root-cut (RC) plots by a trenching method. The daily mean CO<sub>2</sub> efflux values (mean ± 1 standard deviation) were 2.80 ± 2.18, 1.59 ± 1.18, and 1.94 ± 1.58 μmol m<sup>-2</sup> s<sup>-1</sup> in the CT, FT, and RC plots, respectively. Daily mean CO<sub>2</sub> efflux increased exponentially as the groundwater level or water-filled pore space decreased, indicating that oxidative peat decomposition and gas diffusion in the soil increased due to enhanced aeration resulting from lower groundwater levels. Mean annual gap-filled CO<sub>2</sub> emissions were 1.03 ± 0.53, 0.59 ± 0.26, and 0.69 ± 0.21 kg C m<sup>-2</sup> yr<sup>-1</sup> in the CT, FT, and RC plots, respectively. Soil CO<sub>2</sub> emissions were significantly higher in the CT plots (*P* < 0.05), but did not differ significantly between the FT and RC plots. This implies that root respiration was negligible in the FT plots. Heterotrophic respiration accounted for 66% of soil respiration. Annual CO<sub>2</sub> emissions through both soil and heterotrophic respiration were smaller than those of other oil palm plantations on tropical peat, possibly due to the higher groundwater levels, land compaction, and continuous measurement of soil CO<sub>2</sub> efflux in this study. Mean annual total subsidence was 1.55 to 1.62 cm yr<sup>-1</sup>, of which oxidative peat decomposition accounted for 72 to 74%. In conclusion, water management to raise groundwater levels would mitigate soil CO<sub>2</sub> emissions from oil palm plantations on tropical peatland.

### 1. Introduction

Peatland stocks approximately one-third of the global terrestrial carbon (C) in 3% of the global terrestrial area (Maltby and Immirzi, 1993), and approximately 25 Mha are in Southeast Asia, especially in Indonesia and Malaysia (Page et al., 2011). However, tropical peatland has been rapidly reclaimed since the 1990s, mainly for oil palm and *Acacia* plantations. By 2015, oil palm plantations had expanded to cover an area of 4.3 Mha on peat in Indonesia and Malaysia (Miettinen et al., 2016). Because the agricultural use of tropical peatland is commonly accompanied by drainage, the aerobic mineralization of peat soil is promoted, resulting in large carbon dioxide (CO<sub>2</sub>) emissions (e.g.,

Furukawa et al., 2005; Couwenberg et al., 2010; Hooijer et al., 2012). Peat is usually compacted using heavy machinery before planting in Malaysia to enhance its bearing capacity for trees and to increase soil moisture via capillary water rise (Dislich et al., 2016). This compaction practice is expected to depress peat oxidative decomposition due to the increase in soil water content and decrease in soil gas diffusivity (Melling et al., 2005, 2013a).

It has been reported that CO<sub>2</sub> emissions from tropical drained peatland are an important part of the global C cycle (Sjögersten et al., 2014; Miettinen et al., 2017), and therefore it is important to quantify oxidative peat decomposition or heterotrophic respiration (*R<sub>H</sub>*) from total soil respiration (*R<sub>S</sub>*) separately. However, there have been few

\* Corresponding author at: Laboratory of Ecological and Environmental Physics, Research Faculty of Agriculture, Hokkaido University, Kita-ku, Kita 9, Nishi 9, Sapporo, Hokkaido 060-8589, Japan.

E-mail addresses: [ishikura@chem.agr.hokudai.ac.jp](mailto:ishikura@chem.agr.hokudai.ac.jp), [ishikura.kiwamu@gmail.com](mailto:ishikura.kiwamu@gmail.com) (K. Ishikura).

<https://doi.org/10.1016/j.agee.2017.11.025>

Received 8 September 2017; Received in revised form 24 November 2017; Accepted 27 November 2017

0167-8809/© 2017 Elsevier B.V. All rights reserved.

studies of  $R_H$  in tropical peatland, despite  $R_H$  being an important component of  $R_S$  that corresponds to oxidative peat decomposition. For oil palm plantations on peat, some studies have measured  $R_H$  periodically at intervals of one or more months for periods equal to or less than 1 year (Melling et al., 2005, 2013a, 2013b; Dariah et al., 2014; Husnain et al., 2014; Marwanto and Agus, 2014; Sakata et al., 2015; Comeau et al., 2016). Due to the limitations of field studies, the controlling factors of soil  $\text{CO}_2$  efflux are not well understood at the process level. For example, it was reported that no significant relationship exists between  $R_S$  and groundwater level (GWL) (Jauhainen et al., 2008), probably due to the disconnection of capillary force under dry conditions, resulting in soil moisture in the topsoil becoming decoupled from the GWL (Ishikura et al., 2017). Soil moisture in the topsoil can be a better predictor than GWL for soil  $\text{CO}_2$  efflux (Melling et al., 2005, 2013a), because soil moisture is affected more by capillary rise than GWL when a peat soil is compacted (Price, 1997; Michel et al., 2001). However, the relationship between soil  $\text{CO}_2$  efflux and soil moisture in tropical peat ecosystems is still not well understood. For a better understanding, long-term continuous measurement of both  $R_S$  and  $R_H$  is necessary to capture diurnal variation, detect the response of soil  $\text{CO}_2$  efflux to dynamic environmental variations, and reduce the uncertainties in assessment of annual  $\text{CO}_2$  emissions. To our knowledge, no studies have measured  $R_S$  and  $R_H$  continuously in an oil palm plantation on peat.

Oxidative peat decomposition induces subsidence together with physical consolidation and shrinkage (Stephens and Stewart, 1976; Wösten et al., 1997; Hooijer et al., 2012). If the contribution of peat oxidation to total subsidence is determined,  $\text{CO}_2$  emissions through peat decomposition can be estimated from subsidence monitoring (Couwenberg and Hooijer, 2013). However, the extent of this contribution has not yet been determined, because it depends on peat conditions, such as GWL and the time since drainage. Field studies involving simultaneous measurement of peat subsidence and oxidative peat decomposition could enable this to be determined, but only a few studies have been reported (Wakhid et al., 2017).

Therefore,  $R_S$  and  $R_H$  due to oxidative peat decomposition were measured continuously for two years using an automated chamber system, together with GWL, soil moisture, and peat subsidence in an oil palm plantation established on tropical peat. The objectives of this study were to investigate seasonal changes in  $R_S$  and  $R_H$  in relation to soil water conditions, quantify annual cumulative  $R_S$  and  $R_H$  values, and evaluate the contribution of oxidative peat decomposition to subsidence.

## 2. Material and methods

### 2.1. Site description

This study was conducted in an oil palm (*Elaeis guineensis* Jacqu.) plantation (2°11'N, 111°50'E) in a watershed of the Rajang River in Sibul, Sarawak, Malaysia (Fig. 1) at an elevation of approximately 25 m above sea level. The mean annual air temperature and precipitation between 2004 and 2016 were  $26.5 \pm 0.2$  °C and  $2915 \pm 213$  mm yr<sup>-1</sup> (mean  $\pm$  1 standard deviation (SD)), respectively, at the Sungai Salim B meteorological station (Department of Irrigation and Drainage Malaysia), which is 7.4 km from the study site. In September 2004, a mixed peat swamp forest on an ombrotrophic peat dome was converted to an oil palm plantation, with the installation of ditches and water gates; artificial compaction to prevent palms from leaning and toppling was performed during land preparation. The soil type was a Sapric Histosol (IUSS Working Group WRB, 2015), with a peat depth of 12.7 m. Palm seedlings were planted on a triangular grid spacing of 8.5 m between trees (153 trees ha<sup>-1</sup>; Fig. 2), and the ground was sparsely covered by fern plants (*Stenochlaena palustris* (Burm. f.) Bedd.). The lower fronds of oil palm trees were periodically lopped and piled in inter-row spaces. Thus, little leaf litter accumulated on the

ground, except for some areas with fern plants. In 2014, the palm trees were 9 years old, and the canopy height was about 8 m. Oil palm plantations are commonly replanted every 25–30 years (Basiron, 2007), so the study site was in the first cycle of cultivation. The following fertilizers were applied together four times a year (January, March, July–August, and September–October) within 1 m of each stem: 74–147 kg N ha<sup>-1</sup> yr<sup>-1</sup> of urea, 7–9 kg P ha<sup>-1</sup> yr<sup>-1</sup> of rock phosphate, and 239–311 kg K ha<sup>-1</sup> yr<sup>-1</sup> of muriate of potash (KCl). Copper, zinc, and boron were applied as micronutrients at 8–16 kg ha<sup>-1</sup> yr<sup>-1</sup> in May–June every year, and kieserite (MgSO<sub>4</sub>·H<sub>2</sub>O) was also applied at rates of 80 kg ha<sup>-1</sup> in October 2014, 119 kg ha<sup>-1</sup> in May 2015, and 80 kg ha<sup>-1</sup> in January 2016, respectively.

### 2.2. Experimental design and chamber measurement

In April 2014, an experimental area without fern plants was established, and the following treatments were applied (Fig. 2):

Close-to-tree (CT, four plots): distance from the nearest tree < 2.5 m, corresponding to  $R_S$ .

Far-from-tree (FT, four plots): distance from the nearest tree > 3 m, corresponding to  $R_S$ .

Root-cut (RC, four plots): distance from the nearest tree > 3 m with trenching, corresponding to  $R_H$ .

In each RC plot, four stainless steel plates were inserted surrounding an area of 40 × 80 cm<sup>2</sup>. The depth of insertion was 80 cm, which was almost equivalent to the lowest GWL. In May 2014, 1 month later, an automated chamber system was installed in the experimental area. The system consisted of 16 chambers, an infrared  $\text{CO}_2$  analyzer (LI-820, LI-COR, Inc., Lincoln, Nebraska, USA), a programmable data logger (CR1000, Campbell Scientific Inc., Logan, Utah, USA), and an air pump and solenoid valves (Hirano et al., 2009). The chamber consisted of an opaque polyvinyl chloride (PVC) cylinder (height: 40 cm; inner diameter: 25 cm). Chambers were inserted 2–3 cm deep into the soil. One chamber was installed in each CT and FT plot, and two chambers were installed in each RC plot (Fig. 2).

An opaque PVC lid was attached to the chamber top that opened vertically and closed under the control of the data logger. Each chamber closed for 225 s in sequence, one after the other, and it took 1 h for all chambers to close/open in rotation. The air in the headspace of each chamber was circulated through the  $\text{CO}_2$  analyzer when the chambers were closed. The  $\text{CO}_2$  concentration was measured at 10-s intervals and recorded in the data logger. In August 2015, a greenhouse gas analyzer (Ultraportable Greenhouse Gas Analyzer 915-0011, Los Gatos Research, Inc., San Jose, California, USA) was placed in the air circulation line to measure  $\text{CO}_2$ , methane, and water vapor concentrations. Although measurements began in May 2014, data for a two-year period from January 2015 were used, because additional  $\text{CO}_2$  emissions resulting from the decomposition of dead roots left in the trenched plots were expected to occur for several months after trenching (Hanson et al., 2000; Comeau et al., 2016). One palm tree fell on a chamber in a CT plot in August 2015, and the chamber was then moved to an FT position. Thus, the number of CT plots decreased to three, while the number of FT plots increased to five in 2016.  $\text{CO}_2$  data from the  $\text{CO}_2$  analyzer were primarily used; data from the greenhouse gas analyzer were used as an alternative when the LI-820 malfunctioned. During the two years of 2015 and 2016, 23% of the data was lost, mainly due to power problems.

Soil  $\text{CO}_2$  efflux was calculated from the increase in  $\text{CO}_2$  concentration in the chamber headspace during the 90–220 s after the chamber closing:

$$F = \frac{PH}{RT_{\text{air}}} \frac{dC}{dt} \quad (1)$$

where  $F$  is soil  $\text{CO}_2$  efflux ( $\mu\text{mol m}^{-2} \text{s}^{-1}$ ),  $P$  is air pressure (101.325 kPa),  $H$  is the aboveground height of a chamber,  $R$  is the gas constant (8.314 Pa m<sup>3</sup> K<sup>-1</sup> mol<sup>-1</sup>),  $T_{\text{air}}$  is air temperature (K), and  $dC/dt$

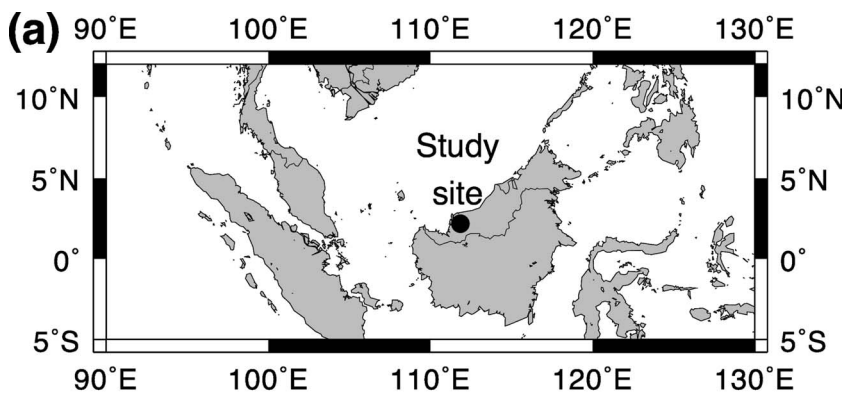


Fig. 1. Map of the study site.

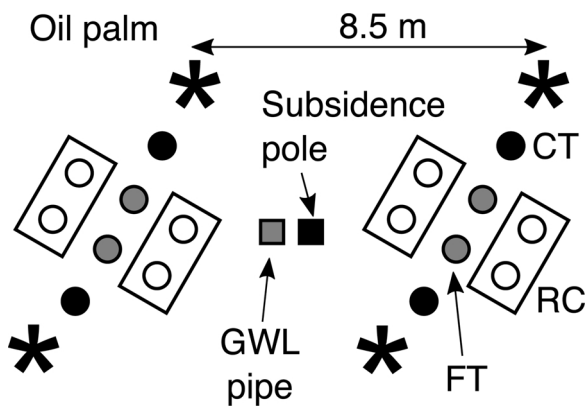
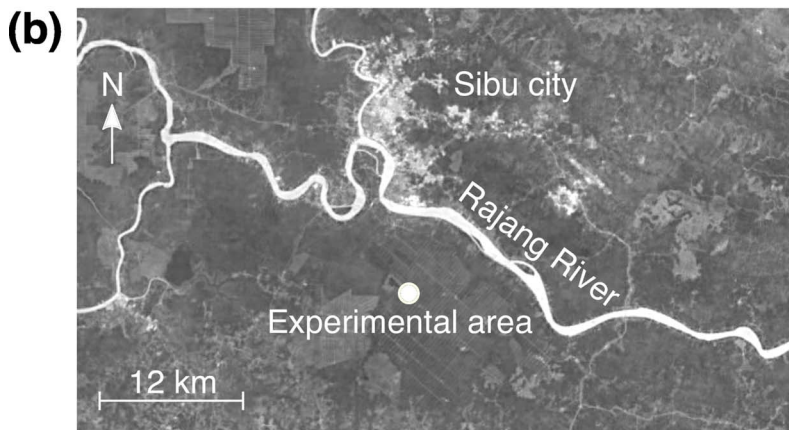


Fig. 2. Allocation of chambers, subsidence pole, and groundwater level (GWL) pipe. CT, FT, and RC represent chamber treatments for close-to-tree (< 2.5 m), far-from-tree (> 3 m), and root-cut plots, respectively.

$dt$  is the rate of increase of the  $\text{CO}_2$  concentration ( $\mu\text{mol mol}^{-1} \text{s}^{-1}$ ). The quality of soil  $\text{CO}_2$  efflux data was controlled as follows:

- 1 Significant slope: the Pearson's correlation coefficient for the rate of increase in the  $\text{CO}_2$  concentration should be higher than 0.661376 ( $P < 0.01, n = 14$ );
- 2 Stationary slope: the rates of increase in  $\text{CO}_2$  concentration from 90 to 150 s and from 160 to 220 s after closing were calculated separately. The difference between the means of the two rates and the rate during the whole period (90–220 s) should be less than 30% (Aguilos et al., 2013);
- 3 Outliers: the  $\text{CO}_2$  flux should be within 0–40  $\mu\text{mol m}^{-2} \text{s}^{-1}$ .

After these quality control criteria were applied, 43% of the data remained available. Because no litter accumulated in any chamber,  $\text{CO}_2$

emissions resulting from leaf litter decomposition were not included in either  $R_S$  or  $R_H$  in this study. The  $\text{CO}_2$  fluxes measured by the two  $\text{CO}_2$  analyzers did not differ significantly from each other (Fig. S1).

### 2.3. Environmental properties

Precipitation was observed at a height of 1 m in an open space about 5 m away from the experimental area. However, some data were lost due to power problems, and precipitation data from the Sungai Salim B meteorological station were therefore used to record annual precipitation. The friction velocity ( $u^*$ ,  $\text{m s}^{-1}$ ) was measured at a height of 21 m above the vegetation canopy using a sonic anemometer (CSAT3, Campbell Scientific Inc.) and was used as an index of atmospheric turbulence.

Air and soil temperatures ( $^{\circ}\text{C}$ ) at a depth of 5 cm were measured using thermocouple thermometers in the same two chambers in FT plots. The GWL (m, negative values represent belowground) was measured using a piezometer (HTV-050KP, Sensez, Tokyo, Japan) at one point (Fig. 2), and volumetric soil water content ( $\text{m}^3 \text{m}^{-3}$ ) at 0–30-cm depth was measured using a time-domain reflectometry (TDR) sensor (CS616, Campbell Scientific Inc.) in FT and RC plots, respectively (Fig. 2). Half-hourly means of these belowground variables were also recorded to the data logger used for the chamber system. Missing daily mean GWLs were gap-filled by a tank model (He and Inoue, 2015). The water retention curve was fitted to the relationship between daily mean GWL and soil water content using van Genuchten's model (van Genuchten, 1980):

$$\theta = \theta_{\text{res}} + \frac{\theta_{\text{sat}} - \theta_{\text{res}}}{(1 + (\alpha h)^n)^{1-1/n}} \tag{2}$$

where  $\theta$  is the soil water content,  $\theta_{\text{sat}}$  is the saturated soil water content (equivalent to the porosity explained below),  $h$  is the pressure head ( $= -100 \times \text{GWL}$ , cm), and  $\alpha$ ,  $n$ , and  $\theta_{\text{res}}$  are fitting parameters,

respectively. Missing daily mean soil water contents were gap-filled from the GWL using the water retention curve (Fig. S3).

In June 2014, six undisturbed soil cores of 100 cm<sup>3</sup> were taken to a depth of 60 cm at intervals of 10 cm using a stainless soil core cylinder. Bulk density (Mg m<sup>-3</sup>) and porosity (m<sup>3</sup> m<sup>-3</sup>) were determined using a digital soil volume analyzer (DIK-1110, Daiki Rika Company, Saitama, Japan). A further three disturbed soil samples were taken to a depth of 60 cm at intervals of 10 cm, and the total C and nitrogen (N) contents (%) were analyzed by the dry combustion method (TruMac CN, LECO Corporation, St. Joseph, Michigan, USA). Other undisturbed soil cores of 100 cm<sup>3</sup> were taken from depths of 0–5, 5–10, 10–20, and 20–30 cm every month during the study period, and the volumetric soil water content was determined using the digital soil volume analyzer. Volumetric soil water content measured by the TDR sensor was calibrated using the soil water content measured by the soil core method. Water-filled pore space (WFPS, m<sup>3</sup> m<sup>-3</sup>) was calculated from the proportion of soil water content to soil porosity.

In February 2017, disturbed topsoil at a depth of 0–30 cm was sampled in four replicate locations around the experimental area. Soil pH (1:2.5H<sub>2</sub>O) was measured using a digital pH meter (827 pH Lab, Metrohm AG, Herisau, Switzerland). Ash content (%) was analyzed by loss-on-ignition (TGA701, LECO Corporation) at 800 °C for more than 1 h. To measure fine root biomass (diameter: < 2 mm), 100 cm<sup>3</sup> soil cores were taken at a depth of 0–10 cm at 1, 2, and 3 m from the four nearest palm trees, respectively. The soil samples were washed and sieved through a 2-mm mesh. Living fine roots were picked out by visual assessment and elasticity, and dried at 75 °C for more than 48 h to measure biomass.

#### 2.4. Subsidence and the contribution of peat decomposition

In May 2014, a subsidence pole with a marking disk was installed vertically into the soil until it reached the mineral soil beneath the peat. Because the measurement height of the pole from the ground surface was affected by the roughness of the ground, the marking disk was used to take an average. The disk could move freely along the anchored pole, and thus was always resting on the ground surface. The heights from the disk on the ground to the top of the pole were measured manually on four sides and averaged every month from June 2014. Annual subsidence was calculated as the cumulative subsidence from January in one year to January in the following year.

Subsidence through oxidative peat decomposition ( $S_{RH}$ , cm period<sup>-1</sup>) was calculated using the following equation (Wakhid et al., 2017):

$$S_{RH} = \frac{\text{Cumulative } R_H}{10 \cdot \text{BD} \cdot \text{TC}} \quad (3)$$

where cumulative  $R_H$  (kg C m<sup>-2</sup> period<sup>-1</sup>) is the cumulative CO<sub>2</sub> emission in RC plots, BD (Mg m<sup>-3</sup>) is bulk density, and TC (g C g<sup>-1</sup>) is the total C content of the soil.

#### 2.5. Data analysis

Nonlinear mixed-effects modeling was applied to analyze the dependencies of the daily mean soil CO<sub>2</sub> efflux (μmol m<sup>-2</sup> s<sup>-1</sup>) on GWL (m) and WFPS (m<sup>3</sup> m<sup>-3</sup>) for each of the CT, FT, and RC plots by fitting the following equations:

$$\text{CO}_2 \text{ efflux} = R_0 \cdot \exp(b \cdot \text{GWL}) \quad (4)$$

$$\text{CO}_2 \text{ efflux} = R_0 \cdot \exp(b \cdot (1 - \text{WFPS})) \quad (5)$$

where  $R_0$  and  $b$  are regression coefficients, and chambers are treated as the random coefficients of  $R_0$  and  $b$ . The residual maximum likelihood (REML) estimation method was used for regression analysis, and the goodness-of-fit was evaluated by the coefficient of determination ( $R^2$ ).

The daily mean soil CO<sub>2</sub> efflux was gap-filled from the daily mean

GWL or WFPS using a regression equation (Eqs. (4) or (5)), and annual cumulative CO<sub>2</sub> emissions were summed for each chamber. The differences in the means of the annual cumulative CO<sub>2</sub> emissions among years (2015 and 2016) and treatments (CT, FT, and RC plots) were tested by a two-way analysis of variance (ANOVA) and a multiple comparison using the Tukey–Kramer method. The ratios of  $R_H$  to  $R_S$  were calculated by dividing the annual soil CO<sub>2</sub> emissions of RC plot by those of CT and FT plots.

Subsidence through the physical processes of shrinkage/swelling and consolidation (cm period<sup>-1</sup>) was determined monthly as the difference between total subsidence and  $S_{RH}$ . It was assumed that physical subsidence ( $S_{phys}$ ) progressed logarithmically over time due to secondary consolidation and fluctuated with GWL by shrinkage/swelling (Eq. (6)). In this simple model, C leaching, especially dissolved organic carbon (DOC) efflux through groundwater discharge (Moore et al., 2011), was incorporated into the first term on the right side. However, the regression of cumulative subsidence over time can be spurious, because cumulative subsidence is probably a unit root process. Therefore, a unit root test (augmented Dickey–Fuller test) was performed for  $S_{phys}$ . As a result,  $S_{phys}$  was significantly stationary ( $P < 0.05$ ) so a linear regression was performed using the following equation:

$$S_{phys} = a \cdot \log_{10}(\text{Days}) + b \cdot (\text{GWL}_i - \text{GWL}_0) \quad (6)$$

where the term Days is the number of days from the beginning of subsidence measurement (June 23, 2014),  $\text{GWL}_0$  is the daily mean GWL on the initial date (= -0.73 m),  $\text{GWL}_i$  is the daily mean GWL when subsidence was measured, and  $a$  and  $b$  are regression coefficients. Because soil CO<sub>2</sub> efflux was available only from January 2015,  $S_{RH}$  in 2014 was estimated from the GWL using Eq. (4). Finally, the smoothed annual total subsidence ( $S_{sm}$ , cm yr<sup>-1</sup>) was calculated using the following equation:

$$S_{sm} = a \cdot \log_{10} \left( \frac{\text{Days}_{y+1}}{\text{Days}_y} \right) + b \cdot (\overline{\text{GWL}}_y - \text{GWL}_0) + S_{RH_y} \quad (7)$$

where  $y$  is the target year (2015 or 2016),  $\text{Days}_y$  is the number of days after January 1 in  $y$  since the beginning of subsidence measurement (June 23, 2014),  $\overline{\text{GWL}}_y$  is the annual mean GWL in  $y$ , and annual  $S_{RH_y}$  is subsidence through  $R_H$  in  $y$ .

All data analyses were conducted using R software (R Core Team, 2017).

### 3. Results

#### 3.1. Environmental properties

The soil pH was  $3.9 \pm 1.0$  (mean  $\pm$  1 SD) and the soil C content was  $52.8 \pm 0.8\%$ ; such a low pH and high C content are typical properties of ombrotrophic peat. Bulk density was  $0.16 \pm 0.04$  Mg m<sup>-3</sup> at a depth of 0–10 cm and  $0.12 \pm 0.02$  Mg m<sup>-3</sup> at a depth of 0–60 cm (Table S1). The ash content was relatively high at  $7.1 \pm 7.9\%$  because of fertilizer applications. Fine root biomass values were  $165 \pm 91$ ,  $86 \pm 63$ , and  $93 \pm 25$  g m<sup>-2</sup> at a depth of 0–10 cm at 1, 2, and 3 m from the nearest tree, respectively.

Annual precipitation amounts in 2015 and 2016 were similar and close to the mean annual precipitation recorded over a 13-year period (2915 mm yr<sup>-1</sup>) (Fig. 3a, Table 1). Daily mean GWL varied from -0.89 to -0.23 m (Fig. S2), with similar annual means in 2015 and 2016 (Fig. 3b, Table 1). The WFPS did not change between 2015 and 2016 (Table 1) and values were similar in the RC and FT plots. No significant difference was found in daily mean soil temperatures between 2015 and 2016 (Table 1).

#### 3.2. Diurnal changes in soil carbon dioxide efflux

Soil temperature at a depth of 5 cm displayed a typical diurnal

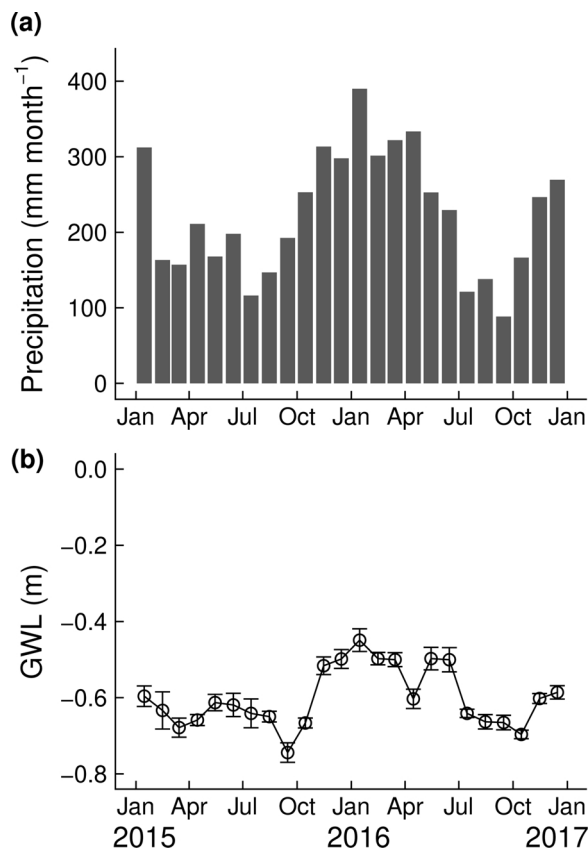


Fig. 3. Variations in (a) monthly precipitation and (b) monthly mean GWL. Error bars denote 95% confidence intervals.

**Table 1**  
Annual sum of precipitation, and annual mean groundwater level (GWL), water-filled pore space (WFPS, 0–30 cm depth) and soil temperature (5 cm depth).

Variables	Treatment	Mean ± 1SD	
		2015	2016
Precipitation (mm yr <sup>-1</sup> )		3000	2910
GWL (m)	FT	-0.62 ± 0.09	-0.57 ± 0.09
WFPS (m <sup>3</sup> m <sup>-3</sup> )	FT	0.70 ± 0.03	0.69 ± 0.03
	RC	0.68 ± 0.03	0.68 ± 0.03
Soil temperature (°C)	FT	26.8 ± 1.5	27.8 ± 2.2

FT: far-from-tree (> 3 m); RC: root-cut.

pattern with a minimum at 7 h and a maximum at 14 h. The diurnal range was about 10 °C (Fig. 4a). Soil temperature was higher than air temperature in the nighttime by about 2 °C on average (Fig. 4a). The  $u^*$  was higher in the daytime than in the nighttime (Fig. 4a). In contrast, soil CO<sub>2</sub> efflux was higher in the nighttime than in the daytime in all treatments (Fig. 4b). Its diurnal pattern was a mirror image of those of temperature and  $u^*$ .

To examine the effects of temperature, soil water condition, and  $u^*$  on diurnal changes in soil CO<sub>2</sub> efflux, a multiple regression was performed for hourly soil CO<sub>2</sub> efflux with soil temperature, GWL, the difference between air and soil temperature ( $\Delta T_{\text{air-soil}}$ , defined as air temperature minus soil temperature), and  $u^*$  as predictors (Table 2). Soil temperature was a significant predictor only in RC plots, while GWL,  $\Delta T_{\text{air-soil}}$ , and  $u^*$  were significant predictors in all treatments. From their standardized regression coefficients,  $\Delta T_{\text{air-soil}}$  was the strongest predictor followed by  $u^*$ , with no general diurnal change expected in GWL. Hourly soil CO<sub>2</sub> efflux was plotted against  $\Delta T_{\text{air-soil}}$  and  $u^*$ , respectively (Fig. 5). Soil CO<sub>2</sub> efflux had a significant negative relationship with  $\Delta T_{\text{air-soil}}$  in each treatment when  $\Delta T_{\text{air-soil}}$  was negative

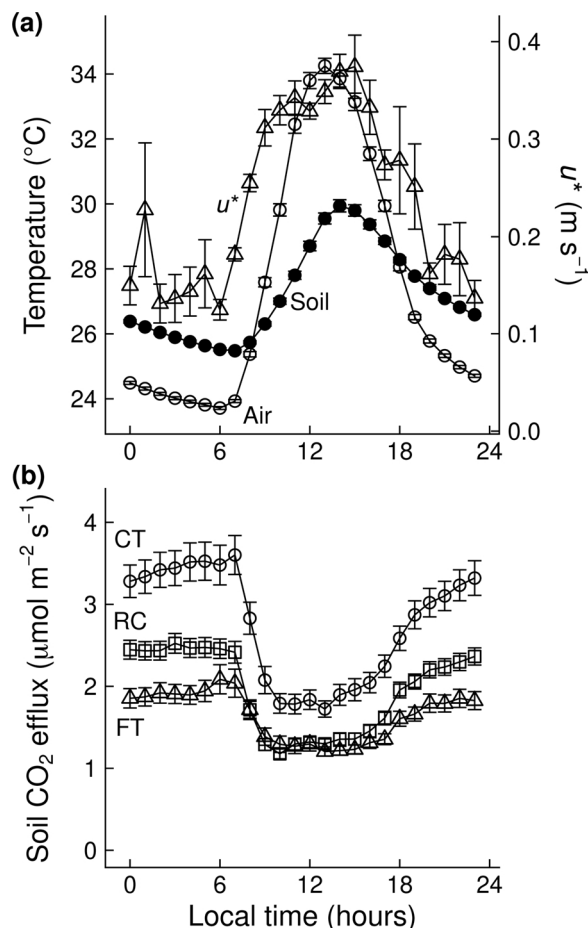


Fig. 4. Diurnal changes in (a) air and soil temperatures and friction velocity ( $u^*$ ) and (b) soil CO<sub>2</sub> flux in the CT, FT, and RC plots. Error bars denote 95% confidence intervals.

**Table 2**  
Results of a multiple regression analysis for hourly soil CO<sub>2</sub> efflux ( $\mu\text{mol m}^{-2} \text{s}^{-1}$ ) with soil temperature (°C), groundwater level (GWL, m), difference between air and soil temperatures ( $\Delta T_{\text{air-soil}}$ ), and friction velocity ( $u^*$ ,  $\text{m s}^{-1}$ ). Std. coeff. represents the standardized regression coefficient.

Treatment	Predictor	Coefficient	Std. coeff.	P-value	R <sup>2</sup>
CT (n = 8618)	Intercept	2.89		< 0.001	0.128
	Soil temperature	-0.03	-0.014	0.18	
	GWL	-10.2	-0.296	< 0.001	
	$\Delta T_{\text{air-soil}}$	-0.20	-0.197	< 0.001	
	$u^*$	-0.57	-0.032	< 0.05	
FT (n = 9506)	Intercept	-2.91		< 0.001	0.107
	Soil temperature	0.07	0.006	0.09	
	GWL	-7.37	-0.303	< 0.001	
	$\Delta T_{\text{air-soil}}$	-0.08	-0.109	< 0.001	
	$u^*$	-0.65	-0.049	< 0.001	
RC (n = 17617)	Intercept	-1.80		< 0.001	0.064
	Soil temperature	0.002	0.001	< 0.001	
	GWL	-6.37	-0.205	< 0.001	
	$\Delta T_{\text{air-soil}}$	-0.11	-0.125	< 0.001	
	$u^*$	-0.92	-0.057	< 0.001	

CT: close-to-tree (< 2.5 m); FT: far-from-tree (> 3 m); RC: root-cut.

(Fig. 5a). A significant negative relationship was found between soil CO<sub>2</sub> efflux and  $u^*$  in each treatment when  $u^*$  was lower than around 0.4  $\text{m s}^{-1}$  (Fig. 5b).

### 3.3. Seasonal changes in soil carbon dioxide efflux

To remove bias due to diurnal changes, the daily mean soil CO<sub>2</sub>

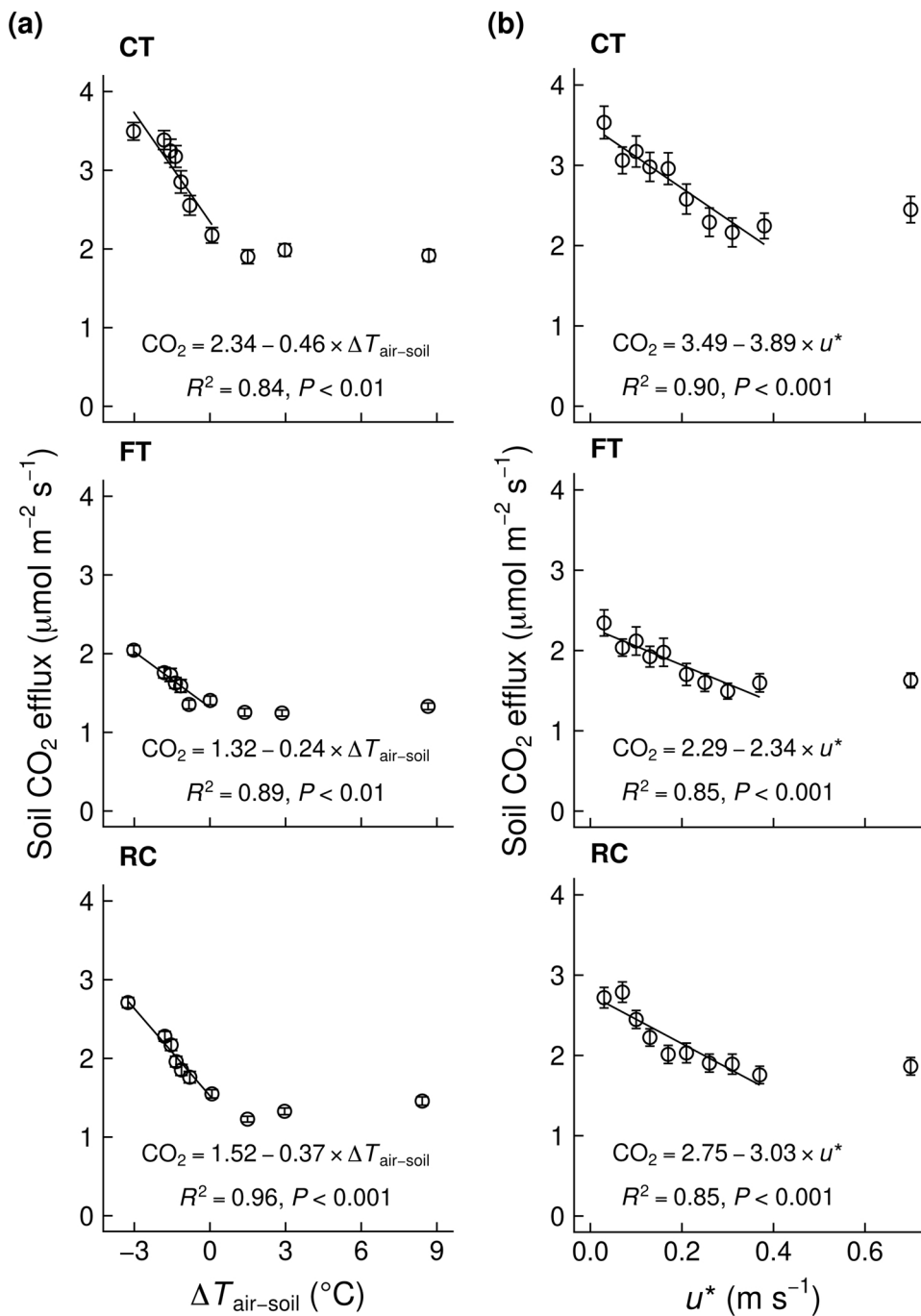


Fig. 5. Relationship of soil CO<sub>2</sub> efflux with the difference between air and soil temperatures ( $\Delta T_{\text{air-soil}}$ , air minus soil) or friction velocity ( $u^*$ ) in the CT, FT, and RC plots. Efflux data were binned into deciles by  $\Delta T_{\text{air-soil}}$  or  $u^*$ . A linear regression was applied to data at  $\Delta T_{\text{air-soil}} < 0$  °C and  $u^* < 0.4$  m s<sup>-1</sup>. Error bars denote 95% confidence intervals.

efflux was calculated only when the number of available data points was larger than six in both the daytime (7–18 h) and nighttime (19–6 h), respectively. The daily mean soil CO<sub>2</sub> efflux values during the two years were  $2.80 \pm 2.18$ ,  $1.59 \pm 1.18$ , and  $1.94 \pm 1.58$   $\mu\text{mol m}^{-2} \text{s}^{-1}$  (mean  $\pm$  1 SD) in the CT, FT, and RC plots, respectively (Fig. 6). Nonlinear mixed-effects models using GWL and WFPS [Eqs. (4) and (5), respectively] were significantly fitted ( $P < 0.001$ ) to daily mean soil CO<sub>2</sub> efflux (Fig. 7). It was found that the daily mean soil CO<sub>2</sub> efflux increased significantly as the GWL or WFPS decreased. The regression with GWL produced higher  $R^2$  values than that with WFPS in the CT and FT plots, while the regression with WFPS produced slightly higher  $R^2$  values than the regression with GWL in RC plots (Fig. 7).

### 3.4. Annual cumulative soil carbon dioxide emission

The daily mean soil CO<sub>2</sub> flux was gap-filled from the GWL using the model (Eq. (4), Fig. 7), and annual sums were calculated (Table 3). Annual cumulative soil CO<sub>2</sub> emissions did not differ between 2015 and 2016 ( $F_{1,27} = 1.59$ ,  $P = 0.22$ ), but differed significantly among the CT, FT, and RC plots ( $F_{2,27} = 4.05$ ,  $P < 0.05$ ). The highest soil CO<sub>2</sub> emission was measured in the CT plots ( $1.03 \pm 0.53$  kg C m<sup>-2</sup> yr<sup>-1</sup>), and the lowest was measured in the FT plots ( $0.59 \pm 0.26$  kg C m<sup>-2</sup> yr<sup>-1</sup>). The  $R_H/R_S$  ratios were 0.66 and 1.16 for RC/CT and RC/FT, respectively (Table 3).

### 3.5. Subsidence

The ground surface subsided, but oscillated in correspondence with

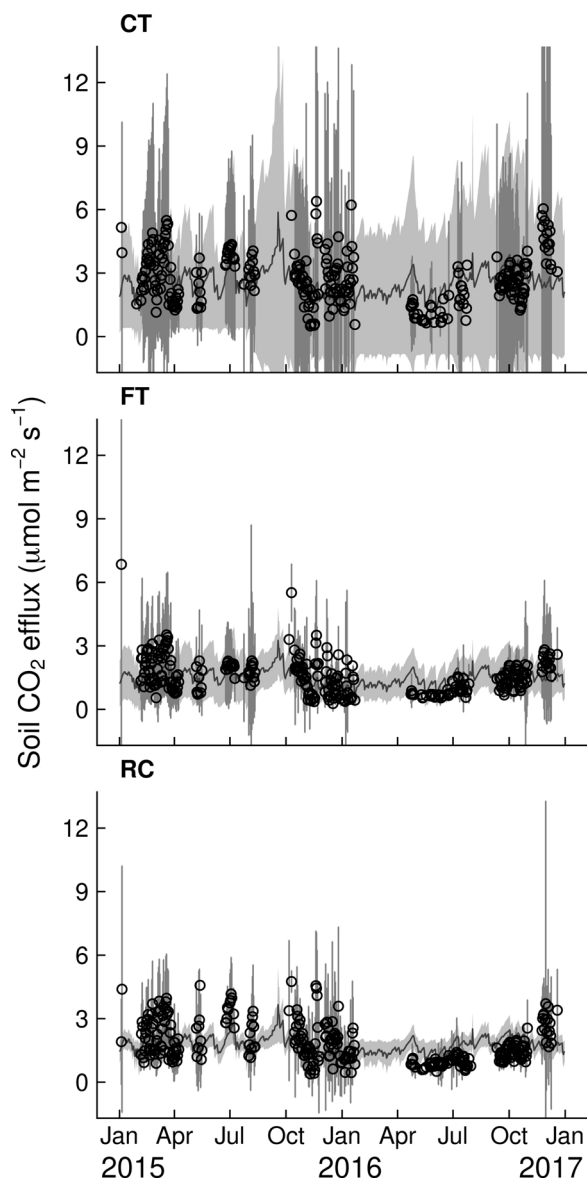


Fig. 6. Seasonal changes in daily mean soil CO<sub>2</sub> efflux in the CT, FT, and RC plots. Circles and lines represent measured and gap-filled values, respectively. Error bars and the gray area denote 95% confidence intervals of measured and estimated soil CO<sub>2</sub> efflux among chambers, respectively.

the GWL (Fig. 8). Total annual subsidence values were determined instantaneously from two measurements in January to be 1.23 and 2.02 cm yr<sup>-1</sup> in 2015 and 2016, respectively (Table 4). The annual  $S_{RH}$  was calculated from the annual  $R_H$ , the bulk density, and C content of 60-cm-thick surface peat using Eq. (3). The result shows that the oxidative subsidence values were 1.22 and 0.99 cm yr<sup>-1</sup> in 2015 and 2016, respectively (Table 4). As a result, the contributions of oxidative peat decomposition to total subsidence were 100 and 49% in 2015 and 2016, respectively, with a mean of 74%.

Physical subsidence ( $S_{phys}$ ) was significantly fitted with Eq. (6) as  $S_{phys} = 1.42 \cdot \log_{10}(\text{Days}) - 6.46 \cdot (\text{GWL}_i + 0.73)$  ( $P < 0.01$ ). The result indicated that the ground subsided physically by 0.65 cm for every GWL lowering of 10 cm. Annual smoothed subsidence ( $S_{sm}$ ) values were 1.83 and 1.27 cm yr<sup>-1</sup>, respectively, in 2015 and 2016. The  $S_{RH}$  accounted for 67 and 78% of the smoothed subsidence in 2015 and 2016, respectively, with a mean of 72% (Table 4).

## 4. Discussion

### 4.1. Factors controlling soil carbon dioxide efflux

Soil CO<sub>2</sub> efflux displayed a clear diurnal pattern that was almost in reverse parallel with soil temperature (Fig. 4). The hourly soil CO<sub>2</sub> efflux had significant negative relationships with GWL,  $\Delta T_{air-soil}$ , and  $u^*$  (Table 1). First, the effects of  $\Delta T_{air-soil}$  and  $u^*$  on the diurnal change in soil CO<sub>2</sub> efflux are considered.

Soil temperature was higher than air temperature at night (Fig. 4a), and soil CO<sub>2</sub> efflux increased significantly as  $\Delta T_{air-soil}$  decreased when  $\Delta T_{air-soil}$  was negative (Table 2, Fig. 5a). Ganot et al. (2014) found that soil CO<sub>2</sub> efflux was promoted by the upward mass flow due to thermal convection in porous mineral soils when the soil temperature was higher than the air temperature. In this study, unsaturated peat soil was more porous than mineral soil. Therefore, our results imply that soil CO<sub>2</sub> efflux was promoted by thermal convection in the unsaturated peat profile. Furthermore, the nighttime thermal convection probably decreased soil CO<sub>2</sub> concentrations more than diffusion, which potentially suppressed soil CO<sub>2</sub> efflux during the following daytime period under stable thermal conditions. On the other hand, Lai et al. (2012) reported that soil CO<sub>2</sub> flux was underestimated by the closed chamber method during periods with a high  $u^*$  in boreal peatland because wind pumps out the soil air just below the ground surface, which decreases the soil CO<sub>2</sub> concentration. The chamber method can measure only the diffusive CO<sub>2</sub> efflux in the closed space, but cannot measure the CO<sub>2</sub> mass flow due to atmospheric turbulence. In this study, the hourly soil CO<sub>2</sub> efflux decreased significantly as  $u^*$  increased (Fig. 5b), which may have led to an underestimation of soil CO<sub>2</sub> efflux in the daytime when  $u^*$  was high on average (Fig. 4a). Therefore, the diurnal change probably resulted from the combination of an increased flux in the nighttime due to thermal convection, a decreased flux in the daytime due to the after-effect of nighttime thermal convection, and an underestimated flux in the daytime due to pumping by atmospheric turbulence. In the calculation of the daily soil CO<sub>2</sub> efflux, the positive and negative effects of thermal convection can be compensated for by making continuous measurements, although some underestimation due to mass flow through pumping is inevitable in a porous soil when the chamber method is applied, especially in unsaturated peat soils.

Soil CO<sub>2</sub> flux increases with soil temperature. The diurnal changes in soil temperature at a depth of 5 cm, with a diurnal range of about 5 °C (Fig. 4a), could have had a positive effect on soil CO<sub>2</sub> efflux. However, the effect of soil temperature was not significant in the CT and FT plots (Table 2). The effect of soil temperature was weaker than that of the other environmental properties in the RC plots, although it was significant due to the large sample size (Table 2). Oxidative peat decomposition would have occurred within the 60-cm deep unsaturated peat horizon because the annual mean GWL was about -0.6 m (Table 1). Thus, soil CO<sub>2</sub> efflux resulting from the total peat decomposition was not directly related to soil temperature, which was similar to the oxidative peat decomposition observed in a burnt ex-peat swamp forest in Central Kalimantan, Indonesia (Hirano et al., 2014).

The effects of GWL and WFPS on the daily mean soil CO<sub>2</sub> efflux were then considered. The soil CO<sub>2</sub> flux had a negative exponential relationship with the GWL in all treatments (Fig. 7), which indicates that soil CO<sub>2</sub> efflux was promoted by lowering of the GWL. A negative relationship between soil CO<sub>2</sub> efflux and GWL has been reported in various tropical peatlands (Furukawa et al., 2005; Hirano et al., 2009, 2014; Couwenberg et al., 2010; Sundari et al., 2012; Ishikura et al., 2017), indicating that peat decomposition is promoted by lowering of the GWL. Lowering of the GWL decreases WFPS and enhances aeration of the soil. As a result, oxidative mineralization of organic matter and gas diffusivity in the soil is accelerated, resulting in increased soil CO<sub>2</sub> efflux (Linn and Doran, 1984). The relationship between soil CO<sub>2</sub> efflux and WFPS in the 30-cm-thick surface peat was also significant, but was weaker than the relationship with GWL in the CT and FT plots, while

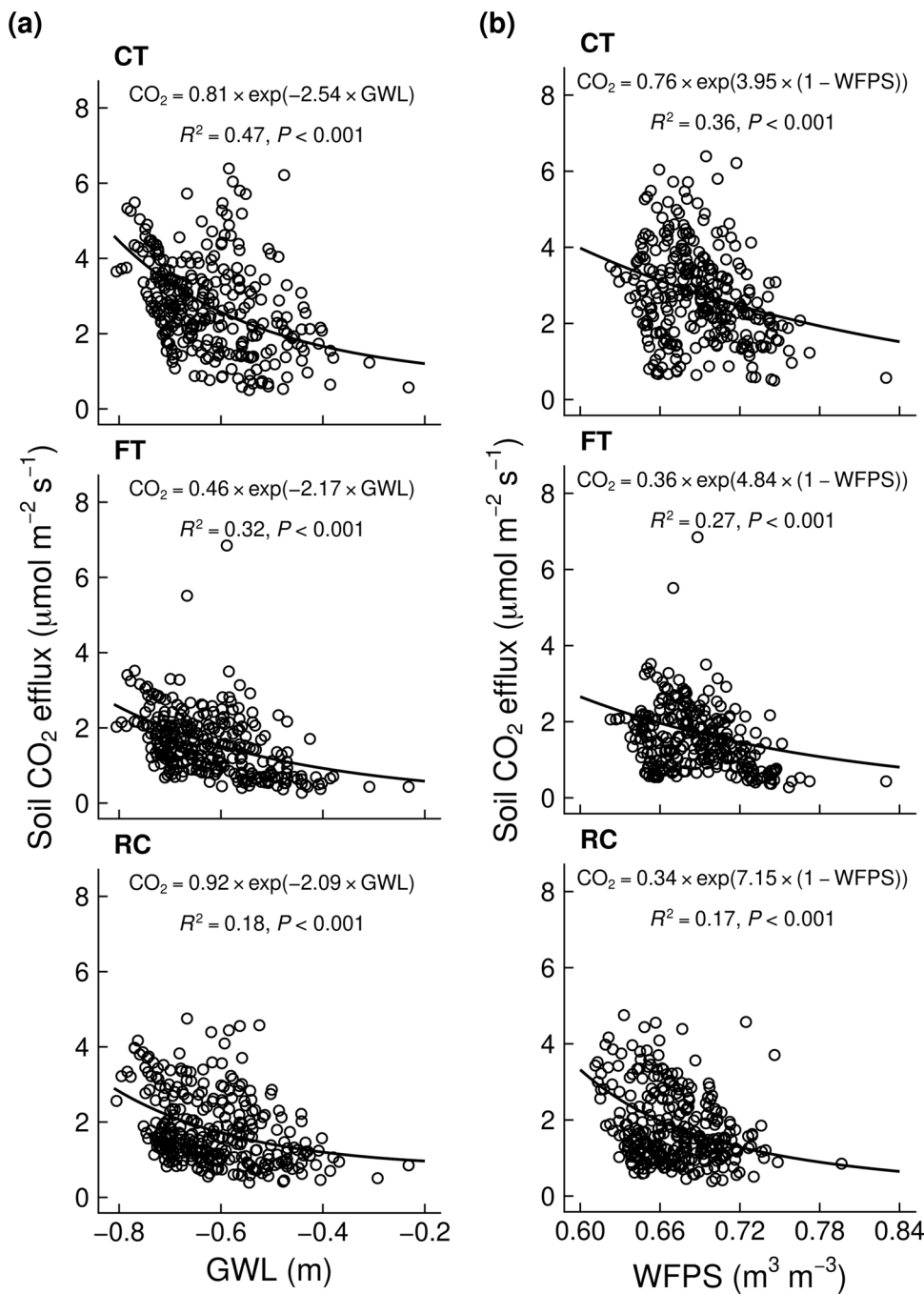


Fig. 7. Relationships of daily mean soil CO<sub>2</sub> efflux with (a) GWL and (b) water-filled pore space (WFPS) in the CT, FT, and RC plots.

Table 3

Annual cumulative soil CO<sub>2</sub> emissions (mean ± 1 standard deviation (n)) and the ratio of heterotrophic to total soil respiration (R<sub>H</sub>/R<sub>S</sub>). Mean values with the same letter are not significantly different (P > 0.05).

Year	Annual cumulative soil CO <sub>2</sub> emission (kg C m <sup>-2</sup> yr <sup>-1</sup> )			R <sub>H</sub> /R <sub>S</sub> ratio	
	CT (R <sub>S</sub> )	FT (R <sub>S</sub> )	RC (R <sub>H</sub> )	RC/CT	RC/FT
2015	1.13 ± 0.63 (3)	0.63 ± 0.30 (4)	0.76 ± 0.24 (8)	0.68	1.20
2016	0.94 ± 0.53 (3)	0.55 ± 0.25 (5)	0.61 ± 0.16 (8)	0.65	1.12
Mean	1.03 ± 0.53 b	0.59 ± 0.26 a	0.69 ± 0.21 ab	0.66	1.16

CT: close-to-tree (< 2.5 m); FT: far-from-tree (> 3 m); RC: root-cut.

the relationships were similar in the RC plots (Fig. 7). In contrast, Ishikura et al. (2017) suggested that WFPS might be better able to explain the variation in peat soil CO<sub>2</sub> efflux than GWL in Central Kalimantan, Indonesia, because disconnection of the capillary force

between surface soil water and groundwater occurred under dry conditions. However, at the site used in the current study, such a disconnection probably did not occur (Fig. S3) because GWL was controlled by water gates and remained relatively high. Melling et al.



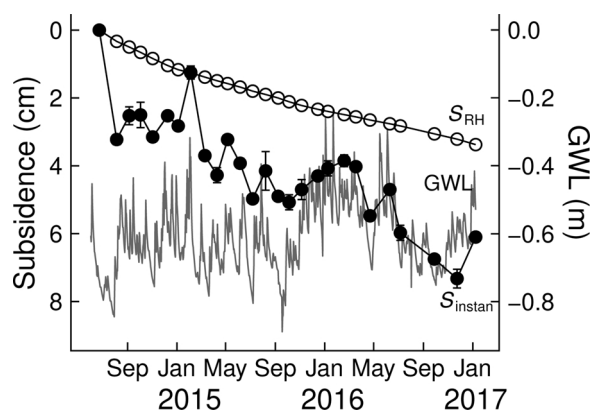


Fig. 8. Cumulative instantaneous total subsidence ( $S_{\text{instant}}$ , closed circles), cumulative oxidative subsidence ( $S_{\text{RH}}$ , open circles) and daily mean GWL (gray line). Error bars denote 95% confidence intervals.

(2013a) found that WFPS was a better predictor of soil  $\text{CO}_2$  efflux than was GWL over a WFPS range of  $0.6\text{--}0.9\text{ m}^3\text{ m}^{-3}$ . However, in the current study the range was narrower ( $0.60\text{--}0.75\text{ m}^3\text{ m}^{-3}$ ), although the GWLs were similar between this study and that of Melling et al. (2013a). The bulk density in Melling et al. (2013a) was higher ( $0.21\text{--}0.23\text{ Mg m}^{-3}$ ) than that recorded in this study (Table 4, S1). Therefore, the effect of a capillary rise on WFPS might have been higher in Melling et al. (2013a) than in this study due to the higher bulk density and lower porosity. These are reasons why WFPS was not a better predictor than GWL in this study.

#### 4.2. Annual cumulative carbon dioxide emission

In this study, 57% of the data from continuous  $\text{CO}_2$  flux measurements during the two years was lost due to power problems and quality controls. To calculate annual cumulative  $\text{CO}_2$  emissions, the data gaps were filled on a daily basis from GWL using negative exponential equations (Fig. 7). Although gap filling causes uncertainties in the assessment of annual emissions, these uncertainties are limited because the seasonal variation in GWL was not large at this study site (Fig. 3b, S2). The annual values are expected to be more reliable than those reported in previous studies, because previous studies estimated annual values from data collected at intervals of one month or longer.

Annual soil  $\text{CO}_2$  emission was significantly larger from the CT plots than from the RC plots, and  $R_{\text{H}}$  accounted for 66% of  $R_{\text{S}}$  (Table 3). In contrast, the annual soil  $\text{CO}_2$  emission from the FT plots did not differ significantly from that of the RC plots (Table 3). Dariah et al. (2014) measured soil  $\text{CO}_2$  efflux at different distances from tree stems in an oil palm plantation on tropical peat and reported that root respiration was negligible at distances of more than 3 m. The distance of each FT plot from the nearest palm tree was greater than 3 m. Thus, the soil  $\text{CO}_2$  efflux in the FT plots was mostly derived from  $R_{\text{H}}$ , and root respiration was probably negligible.

The Intergovernmental Panel on Climate Change (IPCC, 2014)

Table 4

Annual subsidence as a result of oxidative peat decomposition ( $R_{\text{H}}$ ) and its contribution to total subsidence. Bulk density and total carbon (C) content of surface peat with 60-cm thickness are shown. The total annual subsidence rate was determined instantaneously from January's measurements and smoothed using Eq. (7). Values are shown as means  $\pm$  1 standard deviation.

Year	Annual $R_{\text{H}}$	Bulk density	Total C content	Subsidence through $R_{\text{H}}$	Total subsidence rate		Contribution of $R_{\text{H}}$ to subsidence	
	( $\text{kg C m}^{-2}\text{ yr}^{-1}$ )				( $\text{Mg m}^{-3}$ )	(%)	( $\text{cm yr}^{-1}$ )	( $\text{cm yr}^{-1}$ )
2015	$0.76 \pm 0.24$	$0.12 \pm 0.02$	$52.8 \pm 0.8$	$1.22 \pm 0.45$	instantaneous $1.23 \pm 0.49$	smoothed $1.83$	instantaneous 100	smoothed 67
2016	$0.61 \pm 0.16$			$0.99 \pm 0.32$	$2.02 \pm 0.44$	$1.27$	49	78
Mean	$0.69 \pm 0.21$			$1.11 \pm 0.39$	$1.62 \pm 0.46$	$1.55$	74	72

provides a default  $\text{CO}_2$  emission factor of  $1.1\text{ kg C m}^{-2}\text{ yr}^{-1}$ , with 95% confidence intervals of  $0.56\text{--}1.7\text{ kg C m}^{-2}\text{ yr}^{-1}$ , from tropical peat in oil palm plantations for their Tier 1 methodology, although this value was derived from results obtained by the closed chamber and subsidence methods. The annual  $R_{\text{H}}$  measured in the RC plots was almost equivalent to the bottom 95% confidence interval of the Tier 1 method. The annual  $R_{\text{S}}$  in the CT plots was lower than the range of  $1.22\text{--}1.81\text{ kg C m}^{-2}\text{ yr}^{-1}$  reported in previous studies conducted in oil palm plantations on peat (Melling et al., 2005, 2013b; Dariah et al., 2014; Sakata et al., 2015). The annual  $R_{\text{H}}$  was lower than the previously reported range of  $0.69\text{--}1.80\text{ kg C m}^{-2}\text{ yr}^{-1}$  (Melling et al., 2013b; Dariah et al., 2014; Husnain et al., 2014; Marwanto and Agus, 2014). The low  $R_{\text{S}}$  and  $R_{\text{H}}$  in this study may have been caused by the higher annual mean GWL ( $-1.24$  to  $-0.58\text{ m}$ ) than reported in previous studies (Table 1) and by the exclusion of leaf litter decomposition. In addition, previous studies calculated annual soil  $\text{CO}_2$  emissions either by linear interpolation of the monthly  $\text{CO}_2$  flux (Melling et al., 2005, 2013b; Sakata et al., 2015) or by simply averaging periodic  $\text{CO}_2$  flux measurements for less than 1 year (Dariah et al., 2014; Husnain et al., 2014; Marwanto and Agus, 2014), whereas in this study annual  $\text{CO}_2$  emissions were calculated from the quality controlled continuous flux, and data gaps were filled using continuous GWL data. The difference in the calculation methods used would also affect the reported annual soil  $\text{CO}_2$  emissions. The contribution of oxidative peat decomposition to total soil respiration calculated as RC/CT (Table 3) was comparable with the range of 60–86% reported in other oil palm plantations on tropical peat (Dariah et al., 2014; Comeau et al., 2016), except for 38% in Melling et al. (2013a, 2013b).

When considering other land uses on tropical peat, the  $R_{\text{S}}$  in this study was lower than the values of  $1.23$  and  $1.35\text{ kg C m}^{-2}\text{ yr}^{-1}$  reported in swamp forests (Sundari et al., 2012),  $1.68\text{--}4.20\text{ kg C m}^{-2}\text{ yr}^{-1}$  reported in an *Acacia* plantation (Jauhiainen et al., 2012),  $3.29\text{ kg C m}^{-2}\text{ yr}^{-1}$  reported in a rubber plantation (Wakhid et al., 2017), and  $1.11\text{--}1.60\text{ kg C m}^{-2}\text{ yr}^{-1}$  reported in a sago palm plantation (Melling et al., 2005, 2013b). The  $R_{\text{H}}$  in this study was also lower than the ranges of  $0.70\text{--}0.83\text{ kg C m}^{-2}\text{ yr}^{-1}$  reported in swamp forests (Itoh et al., 2017),  $1.91\text{--}3.78\text{ kg C m}^{-2}\text{ yr}^{-1}$  reported in an *Acacia* plantation (Jauhiainen et al., 2012), and the value of  $1.41\text{ kg C m}^{-2}\text{ yr}^{-1}$  reported in a rubber plantation (Wakhid et al., 2017), while it was similar to the range of  $0.60\text{--}0.76\text{ kg C m}^{-2}\text{ yr}^{-1}$  reported in sago palm plantations (Melling et al., 2005, 2013b; Watanabe et al., 2009). In *Acacia* plantations, GWL tends to be lower than in oil palm plantations (Hergoualc'h and Verchot, 2011), which would enhance oxidative peat decomposition.

#### 4.3. Subsidence

The annual total subsidence that was determined instantaneously was higher in 2016 than in 2015, whereas the annual smoothed subsidence was higher in 2015 (Table 4); the interannual difference was larger for instantaneous subsidence. Instantaneous subsidence was calculated simply from two measurements at annual intervals, and therefore was dependent on peat surface oscillation due to short-term

variations in GWL. Therefore, the smaller instantaneous subsidence in 2015 was caused by the higher GWL in January 2016 (Fig. 8). In addition, the interannual order of instantaneous subsidence (2015 < 2016) was inconsistent with that of annual  $R_H$  (2015 > 2016) (Table 4). Because such surface oscillation due to short-term GWL variation was excluded in the smoothed subsidence, annual values reflected the interannual variation in GWL (Table 1) and their order of magnitude was consistent with that of the annual  $R_H$  (2015 > 2016). However, the means of annual subsidence for the two years were similar in the two approaches.

The annual total subsidence in this study (Table 4) was lower than the range of 2.0–5.4 cm yr<sup>-1</sup> reported in previous studies of oil palm plantations on peat (Wösten et al., 1997; Hooijer et al., 2012; Couwenberg and Hooijer, 2013), and was also lower than the 5 cm yr<sup>-1</sup> in an *Acacia* plantation (Hooijer et al., 2012) and 5.96 cm yr<sup>-1</sup> in a rubber plantation (Wakhid et al., 2017) on tropical peat. These studies reported a higher oxidative peat decomposition of 0.69–2.13 kg C m<sup>-2</sup> yr<sup>-1</sup> than was found in this study, which probably resulted in higher subsidence. Previous studies in tropical peatland also reported a lower bulk density of 0.12–0.14 Mg m<sup>-3</sup> than was found in this study, except for the value of 0.24 Mg m<sup>-3</sup> reported by Wakhid et al. (2017). Subsidence increases bulk density, and an increased bulk density decreases subsidence (van Asselen, 2011). Thus, the lower subsidence reported in this study was probably attributable to the higher bulk density due to peat compaction during land preparation before planting.

Peat oxidation accounted for 72–74% of total subsidence on an annual basis (Table 4), which was almost in the middle of the 50–92% range reported in previous studies conducted in tropical peatlands (Murayama and Bakar, 1996; Wösten et al., 1997; Hooijer et al., 2012), except for the value of 25% reported in a rubber plantation (Wakhid et al., 2017).

## 5. Conclusions

Soil CO<sub>2</sub> efflux through both soil respiration and oxidative peat decomposition were measured continuously for two years in an oil palm plantation established on tropical peat. From the large amount of continuous data, it was found that soil CO<sub>2</sub> efflux was lower in the daytime. The opposite diurnal variation for soil and air temperatures was attributable to the mass flow of soil air due to thermal convection at night and to atmospheric turbulence in the daytime. This indicates that periodic measurements conducted only in the daytime would lead to underestimation of soil CO<sub>2</sub> efflux. In addition, further studies are necessary to determine the reliability of chamber methods on peat, which is one of the most porous soils.

The environmental controls on soil CO<sub>2</sub> efflux using daily means were analyzed to exclude diurnal variation in CO<sub>2</sub> efflux. As a result, exponential negative relationships were found between soil CO<sub>2</sub> efflux and GWL even under a relatively narrow seasonal variation in GWL due to water management. Annual gap-filled CO<sub>2</sub> emissions through soil respiration and oxidative peat decomposition were both lower than those in other oil palm plantations on tropical peat, possibly due to the higher GWL and peat compaction observed in this study compared to previous studies. Thus, water management to raise the GWL is important to mitigate soil CO<sub>2</sub> emissions from oil palm plantations on tropical peat. The differences among studies could also be due to differences in precipitation patterns, land-use history, or other factors among plantations. Therefore, further field studies are necessary to reduce the uncertainties in the emission factor of CO<sub>2</sub> from oil palm plantations in Southeast Asia's tropical peatland.

## Acknowledgements

The authors would like to thank the staff of Sarawak Tropical Peat Research Institute for their support during the study and Shun-ichi Nakatsubo at the Institute of Low Temperature Science, Hokkaido

University for chamber preparation. Malaysian Meteorological Department (Sarawak branch) and Department of Irrigation and Drainage, Sarawak supported us to provide the meteorological data for this study. This study was supported by the Sarawak State Government and Federal Government of Malaysia. This study was conducted under the Joint Research Program of the Institute of Low Temperature Science, Hokkaido University, and was also supported by the Japan Society for the Promotion of Science (JSPS) KAKENHI (no. 25257401), the Environment Research and Technology Development Fund (no. 2-1504) of the < GS6 > Environmental Restoration and Conservation Agency and the Ministry of the Environment, Japan < /GS67 >, the Asahi Glass Foundation, and a Grant for Environmental Research Projects from The Sumitomo Foundation.

## Appendix A. Supplementary data

Supplementary data associated with this article can be found, in the online version, at <https://doi.org/10.1016/j.agee.2017.11.025>.

## References

- Aguilos, M., Takagi, K., Liang, N., Watanabe, Y., Teramoto, M., Goto, S., Takahashi, Y., Mukai, H., Sasa, K., 2013. Sustained large stimulation of soil heterotrophic respiration rate and its temperature sensitivity by soil warming in a cool-temperate forested peatland. *Tellus* 65B, 1–13.
- Basiron, Y., 2007. Palm oil production through sustainable plantations. *Eur. J. Lipid Sci. Technol.* 109, 289–295.
- Comeau, L.-P., Hergoualc, K., Hartill, J., Smith, J., Verchot, L.V., Peak, D., Mohammad, A., 2016. How do the heterotrophic and the total soil respiration of an oil palm plantation on peat respond to nitrogen fertilizer application? *Geoderma* 268, 41–51.
- Couwenberg, J., Hooijer, A., 2013. Towards robust subsidence-based soil carbon emission factors for peat soils in south-east Asia, with special reference to oil palm plantations. *Mires Peat* 12, 1–13.
- Couwenberg, J., Dommain, R., Joosten, H., 2010. Greenhouse gas fluxes from tropical peatlands in south-east Asia. *Glob. Change Biol.* 16, 1715–1732.
- Dariah, A., Marwanto, S., Agus, F., 2014. Root- and peat-based CO<sub>2</sub> emissions from oil palm plantations. *Mitig. Adapt. Strateg. Glob. Change* 19, 831–843.
- Dislich, C., Keyel, A.C., Salecker, J., Kisel, Y., Meyer, K.M., Auliya, M., Barnes, A.D., Corre, M.D., Darras, K., Faust, H., Hess, B., Klasen, S., Knohl, A., Kreft, H., Meijide, A., Nurdiansyah, F., Otten, F., Pe'er, G., Steinebach, S., Tarigan, S., Tölle, M.H., Tscharnkte, T., Wiegand, K., 2016. A review of the ecosystem functions in oil palm plantations, using forests as a reference system. *Biol. Rev.* 49. <http://dx.doi.org/10.1111/brv.12295>.
- Furukawa, Y., Inubushi, K., Ali, M., Itang, A.M., Tsuruta, H., 2005. Effect of changing groundwater levels caused by land-use changes on greenhouse gas fluxes from tropical peat lands. *Nutr. Cycl. Agroecosyst.* 71, 81–91.
- Ganot, Y., Dragila, M.I., Weisbrod, N., 2014. Impact of thermal convection on CO<sub>2</sub> flux across the earth-atmosphere boundary in high-permeability soils. *Agric. For. Meteorol.* 184, 12–24.
- Hanson, P.J., Edwards, N.T., Garten, C.T., Andrews, J.A., 2000. Separating root and soil microbial contributions to soil respiration: a review of methods and observations. *Biogeochemistry* 48, 115–146.
- He, X., Inoue, T., 2015. Peatland Tank Model for evaluation of shallow groundwater table data without height reference from benchmark. *Int. J. Environ. Rural Dev.* 6, 16–21.
- Hergoualc'h, K., Verchot, L.V., 2011. Stocks and fluxes of carbon associated with land use change in Southeast Asian tropical peatlands: a review. *Global Biogeochem. Cycles* 25. <http://dx.doi.org/10.1029/2009GB003718>.
- Hirano, T., Jauhiainen, J., Inoue, T., Takahashi, H., 2009. Controls on the carbon balance of tropical peatlands. *Ecosystems* 12, 873–887.
- Hirano, T., Kusin, K., Limin, S., Osaki, M., 2014. Carbon dioxide emissions through oxidative peat decomposition on a burnt tropical peatland. *Glob. Change Biol.* 20, 555–565.
- Hooijer, A., Page, S., Jauhiainen, J., Lee, W.A., Lu, X.X., Idris, A., Anshari, G., 2012. Subsidence and carbon loss in drained tropical peatlands. *Biogeosciences* 9, 1053–1071.
- Husnain, H., Wigena, I.G.P., Dariah, A., Marwanto, S., Setyanto, P., Agus, F., 2014. CO<sub>2</sub> emissions from tropical drained peat in Sumatra: Indonesia. *Mitig. Adapt. Strateg. Glob. Change* 19, 845–862.
- IPCC, 2014. 2013 Supplement to the 2006 IPCC Guidelines for National Greenhouse Gas Inventories. IPCC, Wetlands. Switzerland.
- IUSS Working Group WRB, 2015. World Reference Base for Soil Resources 2014, update 2015 International soil classification system for naming soils and creating legends for soil maps. *World Soil Resources Reports No. 106*. FAO, Rome.
- Ishikura, K., Yamada, H., Toma, Y., Takakai, F., Morishita, T., Darung, U., Limin, A., Limin, S.H., Hatano, R., 2017. Effect of groundwater level fluctuation on soil respiration rate of tropical peatland in Central Kalimantan Indonesia. *Soil Sci. Plant Nutr.* 63, 1–13.
- Itoh, M., Okimoto, Y., Hirano, T., Kusin, K., 2017. Factors affecting oxidative peat decomposition due to land use in tropical peat swamp forests in Indonesia. *Sci. Total*

- Environ. 609, 906–915.
- Jauhainen, J., Limin, S., Silvennoinen, H., Vasander, H., 2008. Carbon dioxide and methane fluxes in drained tropical peat before and after hydrological restoration. *Ecology* 89, 3503–3514.
- Jauhainen, J., Hooijer, A., Page, S.E., 2012. Carbon dioxide emissions from an *Acacia* plantation on peatland in Sumatra Indonesia. *Biogeosciences* 9, 617–630.
- Lai, D.Y.F., Roulet, N.T., Humphreys, E.R., Moore, T.R., Dalva, M., 2012. The effect of atmospheric turbulence and chamber deployment period on autochamber CO<sub>2</sub> and CH<sub>4</sub> flux measurements in an ombrotrophic peatland. *Biogeosciences* 9, 3305–3322.
- Linn, D.M., Doran, J.W., 1984. Effect of water-filled pore space on carbon dioxide and nitrous oxide production in tilled and nontilled soils. *Soil Sci. Soc. Am. J.* 48, 1267.
- Maltby, E., Immirzi, P., 1993. Carbon dynamics in peatlands and other wetland soils regional and global perspectives. *Chemosphere* 27, 999–1023.
- Marwanto, S., Agus, F., 2014. Is CO<sub>2</sub> flux from oil palm plantations on peatland controlled by soil moisture and/or soil and air temperatures? *Mitig. Adapt. Strateg. Glob. Change* 19, 809–819.
- Melling, L., Hatano, R., Goh, K.J., 2005. Soil CO<sub>2</sub> flux from three ecosystems in tropical peatland of Sarawak, Malaysia. *Tellus* 57B, 1–11.
- Melling, L., Goh, K.J., Chaddy, A., Hatano, R., 2013a. Soil CO<sub>2</sub> fluxes from different ages of oil palm in tropical peatland of Sarawak, Malaysia as influenced by environmental and soil properties. *Acta Hort.* 982, 25–35.
- Melling, L., Yun Tan, C.S., Goh, K.J., Hatano, R., 2013b. Soil microbial and root respirations from three ecosystems in tropical peatland of Sarawak Malaysia. *J. Oil Palm Res.* 25, 44–57.
- Michel, J.C., Rivière, L.M., Bellon-Fontaine, M.N., 2001. Measurement of the wettability of organic materials in relation to water content by the capillary rise method. *Eur. J. Soil Sci.* 52, 459–467.
- Miettinen, J., Shi, C., Liew, S.C., 2016. Land cover distribution in the peatlands of Peninsular Malaysia, Sumatra and Borneo in 2015 with changes since 1990. *Glob. Ecol. Conserv.* 6, 67–78.
- Miettinen, J., Hooijer, A., Vernimmen, R., Liew, S.C., Page, S.E., 2017. From carbon sink to carbon source: extensive peat oxidation in insular Southeast Asia since 1990. *Environ. Res. Lett.* 12, 24014.
- Moore, S., Gauci, V., Evans, C.D., Page, S.E., Hall, W., Keynes, M., Wales, E.C., Road, D., 2011. Fluvial organic carbon losses from a Bornean blackwater river. *Biogeosciences* 8, 901–909.
- Murayama, S., Bakar, Z.A., 1996. Decomposition of tropical peat soils. 2. Estimation of in situ decomposition by measurement of CO<sub>2</sub> flux. *Japan Agric. Res. Q* 30, 153–158.
- Page, S.E., Rieley, J.O., Banks, C.J., 2011. Global and regional importance of the tropical peatland carbon pool. *Glob. Change Biol.* 17, 798–818.
- Price, J., 1997. Soil moisture, water tension, and water table relationships in a managed cutover bog. *J. Hydrol.* 202, 21–32.
- R Core Team, 2017. *R: A Language and Environment for Statistical Computing*. R Foundation for Statistical Computing. R Core Team, Vienna, Austria. <https://www.r-project.org/>.
- Sakata, R., Shimada, S., Arai, H., Yoshioka, N., Yoshioka, R., Aoki, H., Kimoto, N., Sakamoto, A., Melling, L., Inubushi, K., 2015. Effect of soil types and nitrogen fertilizer on nitrous oxide and carbon dioxide emissions in oil palm plantations. *Soil Sci. Plant Nutr.* 61, 48–60.
- Sjögersten, S., Black, C.R., Evers, S., Hoyos-Santillan, J., Wright, E.L., Turner, B.L., 2014. Tropical wetlands: a missing link in the global carbon cycle? *Global Biogeochem. Cycles* 28, 1371–1386.
- Stephens, J.C., Stewart, E.H., 1976. Effect of climate on organic soil subsidence. In: *Proceedings of the 2nd Symposium on Land Subsidence*. Anaheim California. pp. 647–655.
- Sundari, S., Hirano, T., Yamada, H., Kusin, K., Limin, S., 2012. Effect of groundwater level on soil respiration in tropical peat swamp forests. *J. Agric. Meteorol.* 68, 121–134.
- Wösten, J.H.M., Ismail, A.B., van Wijk, A.L.M., 1997. Peat subsidence and its practical implications: a case study in Malaysia. *Geoderma* 78, 25–36.
- Wakhid, N., Hirano, T., Okimoto, Y., Nurzakiah, S., Nursyamsi, D., 2017. Soil carbon dioxide emissions from a rubber plantation on tropical peat. *Sci. Total Environ.* 581–582, 857–865.
- Watanabe, A., Purwanto, B.H., Ando, H., Kakuda, K., Jong, F.-S., 2009. Methane and CO<sub>2</sub> fluxes from an Indonesian peatland used for sago palm (*Metroxylon sagu* Rottb.) cultivation: effects of fertilizer and groundwater level management. *Agric. Ecosyst. Environ.* 134, 14–18.
- van Asselen, S., 2011. The contribution of peat compaction to total basin subsidence: implications for the provision of accommodation space in organic-rich deltas. *Basin Res.* 23, 239–255.
- van Genuchten, M.T., 1980. A closed-form equation for predicting the hydraulic conductivity of unsaturated soils. *Soil Sci. Soc. Am. J.* 44, 892–898.